Structural and acoustical wave interaction at a wedge-shaped junction of fluid-loaded plates

A. N. Norris
Department of Mechanical and Aerospace Engineering, Rutgers University, Piscataway, New Jersey 08855

A. V. Osipov
Institute of Radiophysics, The St. Petersburg State University, Uljanovskaja 1-1, Petrodvorets 198904, Russia

(Received 4 March 1996; accepted for publication 4 October 1996)

Two semi-infinite elastic plates are joined along a line forming a wedge structure with unilateral fluid loading in the outer sector of the two plates. The structure is modeled using thin plate theory, allowing freely propagating flexural and longitudinal waves. The junction is mechanically connected with an applied force and moment acting there to simulate a possible internal connection. The general two-dimensional solution is described for incidence of time harmonic structural or acoustical waves. The total pressure is expressed as a Sommerfeld integral, the integrand comprising Malyuzhinets functions and particular solutions of certain difference equations. The junction conditions reduce to a system of four linear equations. Numerical examples indicate the coupling between the modes for welded steel plates in water. Acoustic plane-wave incidence on the flattest junction considered is converted almost equally, in terms of energy, among diffracted flexural and longitudinal waves. The coupling to flexural energy increases with the angle of the water wedge sector, at the expense of the longitudinal energy which vanishes in the limit as the water occupies the entire domain except for a strip comprising the two plates. An incident longitudinal wave generates relatively little acoustic sound for all wedge angles considered, with most of its energy redistributed among structural modes. The acoustical diffraction is generally greater for flexural incidence. Comparison with the dry structural diffraction coefficients indicates that the fluid loading effects for steel and water configurations can be significant for frequencies less than one-fifth of the coincidence frequency, but are small for higher frequencies. [S0001-4966(97)03802-2]

PACS numbers: 43.40.Dx, 43.40.Rj [CBB]

INTRODUCTION

We consider a wedge configuration formed by two elastic plates joined at an angle, with the simplification that the plates are thin and the complication that the structure is loaded unilaterally by an acoustic fluid. The thin plate assumption means that only the basic symmetric and antisymmetric structural modes need to be considered, corresponding to longitudinal and flexural waves. The major difficulty is to simultaneously satisfy the structural dynamic equations and the Helmholtz equation for the acoustic pressure, subject to the continuity conditions at the solid–liquid boundary, and the junction conditions at the vertex. We restrict attention here to the two-dimensional configuration, as depicted in Fig. 1, for which all motion is in the plane normal to the line joining the plates. Our objective is to quantitatively understand the various wave interaction mechanisms, such as structural to structural or acoustic to structural, and the significance of the fluid loading on these interactions.

Similar problems for flat fluid-loaded structural configurations, such as two connected semi-infinite plates[1] or infinite plates with line attachments,[2,3] have been studied in detail. They differ both physically and mathematically from the present situation. First, there is generally no coupling of the longitudinal structural motion with the acoustic and flexural waves. Thus, the in-plane longitudinal motion is completely decoupled. Second, conventional Fourier transform and Wiener–Hopf techniques may be used for problems defined on rectangular coordinates, e.g., Ref. 4, but do not suffice for wedge configurations. The general procedure for solving acoustic diffraction from wedges with higher-order boundary conditions has only recently been developed,[5,6] and has been applied successfully to membrane boundaries,[6,7] and also to plates. Thus, Osipov[8] showed that writing the acoustic field as a Sommerfeld integral transform reduces the plate boundary conditions to functional difference equations for the pressure transform. He also provided an explicit procedure for solving these equations using Malyuzhinets functions and Fourier transforms.

In this paper we discuss the general solution for various contact conditions along the line where the plates meet, including the case of welded contact for which displacements and forces are continuous. This case is of most practical significance, but unfortunately, was not considered by Osipov.[8] The problem involves six continuity conditions at the junction: two for the two velocity components, two more for the force components, and one each for the bending moment and the rotation. We showed in a related paper[9] that the six continuity conditions can be expressed solely in terms of the transverse plate displacement as a set of four conditions. Approximate results appropriate to wedge configurations that are almost flat were also derived in Ref. 9, but the general

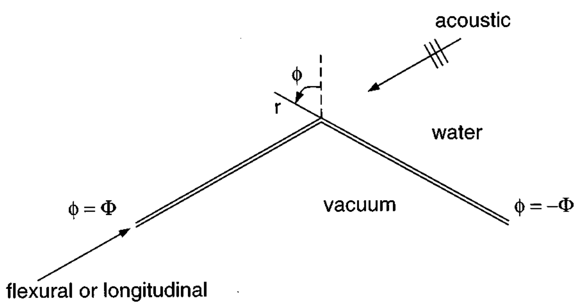

FIG. 1. The wedge configuration.

case was not considered. It is interesting to note that excitation by an incident longitudinal wave produces no forcing in the fluid or flexural equations, but the four junction conditions involve an effective line force at the vertex, the amplitude of which is related to the incident wave amplitude. Thus, longitudinal incidence is equivalent to the radiation problem with a source at the vertex.

The outline of the paper is as follows. The problem is defined in Sec. I, and the general solution procedure based on the Sommerfeld integral transform is described in Sec. II. For a given structure and an incident structural or acoustic wave the problem is reduced to finding eight constants: the values of the normal displacement and its first three derivatives on both plates at the vertex. In Sec. III a system of linear equations for the eight unknowns is obtained by applying appropriate regularity conditions on the Sommerfeld transform and by applying the junction conditions, thus completing the solution. The diffracted structural wave amplitudes are defined and an energy conservation relation is described in Sec. IV. We conclude with a discussion of several illustrative numerical examples in Sec. V.

I. BASIC EQUATIONS

The plate configuration and an incident acoustic wave are depicted in Fig. 1. We are interested in the time harmonic acoustic pressure field $p=p(r,\phi)e^{-i\omega t}$ satisfying the Helmholtz equation outside the wedge,

$$\nabla^2 p+k^2 p=0,\quad 0<r<\infty,\quad -\Phi<\phi<\Phi, \tag{1}$$

where $k=\omega/c$ is the acoustic wave number, and r,ϕ are polar coordinates relative to the contact line. The equations of motion and continuity on the wedge faces are

$$\begin{aligned}&-B_\pm\frac{d^4 w_\pm}{dr^4}+m_\pm\omega^2 w_\pm=p(r,\pm\Phi),\quad 0<r<\infty,\\ &\rho\omega^2 w_\pm(r)=\mp\frac{1}{r}\frac{\partial p}{\partial\phi}(r,\pm\Phi),\quad 0<r<\infty.\end{aligned} \tag{2}$$

Here, $w(r)$ is the displacement into the fluid, and m, B, and ρ are the plate density, bending stiffness, and the fluid density. In general, the plate parameters may be different for each face of the wedge, so we denote them as $w_\pm$, $B_\pm$, $m_\pm$, where $\pm$ signs correspond to the upper ($\phi=\Phi$) and lower ($\phi=-\Phi$) faces, respectively.

At this stage we define some parameters which simplify the analysis later: the plate flexural wave numbers $\kappa_\pm=(m_\pm\omega^2/B_\pm)^{1/4}$, and the nondimensional frequency parameters $\Omega_\pm=k^2/\kappa_\pm^2=\omega/\omega_c^\pm$ where $\omega_c^\pm$ are the plate coincidence frequencies, $\omega_c^\pm=c^2\sqrt{m_\pm/B_\pm}$. The remaining plate dynamics can be represented by frequency independent dimensionless fluid-loading parameters,

$$\epsilon_\pm=\frac{\rho\Omega_\pm}{km_\pm},\quad \delta_\pm=\frac{c_\pm}{c}, \tag{3}$$

where $c_\pm=\sqrt{C_\pm/m_\pm}$ is the longitudinal wave speed and $C_\pm$ is the extensional stiffness. Note that both $\epsilon_\pm$ and $\delta_\pm$ are also independent of the plate thicknesses: thus, for Kirchhoff thin plate theory $\epsilon_\pm=\delta_\pm\rho/(\rho_\pm\sqrt{12})$ and $\delta_\pm=c^{-1}\sqrt{E_\pm/[\rho_\pm(1-\nu_\pm^2)]}$, where $E_\pm$, $\rho_\pm$, and $\nu_\pm$ are Young's modulus, volumetric density and Poisson's ratio, respectively.

The excitation may arise from a variety of sources: (i) an incident acoustic plane wave as shown in Fig. 1,

$$p_i(r,\phi,\phi_0)=P_0\exp[-ikr\cos(\phi-\phi_0)], \tag{4}$$

(ii) an incident subsonic flexural wave on the plate $\phi=\pm\Phi$ is also given by (4) with complex-valued incident angle $\phi_0=\pm(\Phi-\theta_1^\pm)$, where $\theta_1^\pm$ are defined below. Alternatively, (iii) the excitation may be an incident longitudinal wave on either plate,

$$u_\pm^{\rm inc}(r)=U_0^\pm\exp(-i\omega r/c_\pm), \tag{5}$$

where $u_\pm^{\rm inc}(r)$ are the in-plane displacement components of the plates in the radial direction. In order to make the different incident wave types have consistent amplitudes, let $S_0^\pm=\omega kZ_\pm U_0^\pm$, or

$$\omega kZ_\pm u_\pm^{\rm inc}(r)=S_0^\pm\exp(-i\omega r/c_\pm), \tag{6}$$

where $Z_\pm=m_\pm c_\pm$ are the longitudinal wave impedances. Thus, $S_0^\pm$ have the same units (pressure) as P_0. We note that the Poisson effect is ignored here, and consequently the incident longitudinal waves have no pressure in the fluid. They enter the problem explicitly through the junction conditions. We will see that they can be considered by applying an equivalent force at the junction, see (44) below. In general, any one of the three types of incident waves excites all others. The central problem here is to determine the relative coupling amplitudes.

II. GENERAL SOLUTION

A. Field representation and functional equations

We seek the solution in the form of a Sommerfeld integral

$$\begin{aligned}p(r,\phi)&=\frac{1}{2\pi i}\int_\gamma e^{-ikr\cos\alpha}S(\alpha+\phi)d\alpha\\ &=\frac{1}{2\pi i}\int_{\gamma_+}e^{-ikr\cos\alpha}[S(\alpha+\phi)\\ &\quad -S(-\alpha+\phi)]d\alpha.\end{aligned} \tag{7}$$

The contour $\gamma=\gamma_+\cup\gamma_-$, where γ_+ is a loop in the upper half of the complex α plane, beginning at $\pi/2+i\infty$, ending at $-3\pi/2+i\infty$, with $\mathrm{Im}\alpha$ lying above the maximum value of

$|\mathrm{Im}(\theta_n^{\pm})|$, where the complex angles $\theta_n^{\pm}$ $n=1,2,\ldots,5$, are defined below. The contour γ_- is the image of γ_+ under inversion about the origin $\alpha=0$. The "transform" $S(\alpha)$ should be a meromorphic function of a complex variable α, have a single pole with residue P_0 at $\alpha=\phi_0$ in the strip $\Pi_0=\{\alpha:|\mathrm{Re}\ \alpha|\leqslant\Phi\}$ to reproduce the incident field (4), and be bounded when $\mathrm{Im}\alpha\to\pm\infty$ satisfying $S(i\infty)=-S(-i\infty)$ without loss of generality.

The Sommerfeld integral (7) is closely related to the Laplace transform. Define the transform

$$\mathscr{T}[f(r)]\equiv\hat{f}(\alpha)=\frac{i}{2}k\sin\alpha\int_0^{\infty}e^{ikr\cos\alpha}f(r)dr, \tag{8}$$

with inverse transform[10]

$$\mathscr{T}^{-1}[\hat{f}]=f(r)=\frac{1}{2\pi i}\int_{\gamma}e^{-ikr\cos\alpha}\hat{f}(\alpha)d\alpha. \tag{9}$$

Note that $\hat{f}(\alpha)=(i/2)\ k\sin\alpha F(-ik\cos\alpha)$ where $F(s)$ is the Laplace transform of $f(r)$, and

$$\mathscr{T}\left[\frac{df}{dr}(r)\right]=-ik\cos\alpha\hat{f}(\alpha)-\frac{i}{2}k\ \sin\alpha f(0). \tag{10}$$

Equation (7) implies that

$$\hat{p}(\alpha,\phi)=\mathscr{T}[p(r,\phi)]=S(\alpha+\phi), \tag{11}$$

and the transform of the normal displacement is

$$\hat{w}_{\pm}(\alpha)=\pm\frac{ik}{\rho\omega^2}\sin\alpha\,\hat{p}(\alpha,\pm\Phi). \tag{12}$$

The transform of the boundary conditions (2) is therefore, using (10)–(12),

$$\begin{aligned}\mathscr{T}&\left[-B_{\pm}\frac{d^4w_{\pm}}{dr^4}+m_{\pm}\omega^2w_{\pm}-p\right]\\&=L_{\pm}(\alpha)S(\alpha\pm\Phi)+\frac{ik}{2}\sin\alpha\,B_{\pm}[w_{\pm}'''(0)\\&\quad-ik\cos\alpha w_{\pm}''(0)-k^2\cos^2\alpha w_{\pm}'(0)\\&\quad+ik^3\cos^3\alpha w_{\pm}(0)],\end{aligned} \tag{13}$$

where

$$L_{\pm}(\alpha)=\pm i\frac{\Omega_{\pm}}{\epsilon_{\pm}}\sin\alpha(1-\Omega_{\pm}^2\cos^4\alpha)-1. \tag{14}$$

The inverse transform of (13) must be zero for all positive r, implying that the right-hand side of (13) must be an odd function of α. This leads to a pair of functional equations

$$\begin{aligned}L_{\pm}(\alpha)&S(\alpha\pm\Phi)-L_{\pm}(-\alpha)S(-\alpha\pm\Phi)\\&=2\sin\alpha\sum_{n=1}^{4}C_n^{\pm}\cos^{n-1}\alpha,\end{aligned} \tag{15}$$

with constants $C_n^{\pm}$, $n=1,2,3,4$ which depend upon the normal displacement and its derivatives at the tip:

$$C_n^{\pm}=\frac{B_{\pm}}{2}(-ik)^n\frac{d^{4-n}w_{\pm}}{dr^{4-n}}(0). \tag{16}$$

Thus, the problem is reduced to a system of functional equations (15) with eight constants $C_n^{\pm}$, $n=1,2,3,4$, which are to be determined.

B. The plate angles

The general solution depends crucially upon the angles $\theta_n^{\pm}$, Re $\theta_n^{\pm}\in(-\pi/2,\pi/2)$, $n=1,\ldots,5$, defined by

$$L_{\pm}(\mp\theta_n^{\pm})=0, \tag{17}$$

or $\sin\theta_n^{\pm}=X_n^{\pm}$, where $X_n^{\pm}$, $n=1,\ldots,5$ are the roots of the equation $F_{\pm}(X_n^{\pm})=0$, and

$$F_{\pm}(X)=X^5-2X^3-(\Omega_{\pm}^{-2}-1)X+i\epsilon_{\pm}/\Omega_{\pm}^3. \tag{18}$$

By analogy with optics, $\theta_n^{\pm}$ may be interpreted as Brewster angles for each plate. They are related to the structural wave numbers of infinite plates through the connection $\gamma=ik\sin\theta_n^{\pm}$, where γ is the commonly used decay wave number, e.g., Ref. 11. Crighton[12] has examined the root structure of the related fifth-order polynomial equation for γ [Eq. (3.1) of Ref. 12]. Based upon this, we deduce that for real $\Omega_{\pm}$ and $\epsilon_{\pm}$, there exists one and only one root of $F_{\pm}(X_n^{\pm})=0$ on the negative imaginary axis, say $X_1^{\pm}$. The imaginary roots $\theta_1^{\pm}$ have Im $\theta_1^{\pm}<0$ and correspond to a subsonic flexural wave which propagates unattenuated along each plate and decays exponentially into the fluid. Of the four remaining X-roots, two lie in the lower and two in the upper half-plane, symmetrically positioned with respect to the imaginary axis.

The two roots in the upper half-plane, $X_4^{\pm}$ and $X_5^{\pm}$, lie on the imaginary axis if the following inequality is satisfied:

$$\frac{4\Omega_{\pm}^3}{5^{5/2}}\left(\frac{5}{\Omega_{\pm}^2}-2-\sqrt{4+\frac{5}{\Omega_{\pm}^2}}\right)\left(\sqrt{4+\frac{5}{\Omega_{\pm}^2}}-3\right)^{1/2}\geqslant\epsilon_{\pm}. \tag{19}$$

This condition is new (we believe), and may be determined as follows. Let $X=-i\eta$, so that $F_{\pm}(X)=0$ is equivalent to $G_{\pm}(\eta)=0$. The related equation $G_{\pm}'(\eta)=0$ has real roots only if $\Omega_{\pm}\leqslant 1$ and they occur at $\eta=\sqrt{\zeta_{\pm}}$, $\eta=-\sqrt{\zeta_{\pm}}$, where $\zeta_{\pm}=-\frac{3}{5}+\frac{1}{5}(4+5/\Omega_{\pm}^2)^{1/2}$. Since $G_{\pm}(0)<0$ and $G_{\pm}(\eta)\to\pm\infty$ as $\eta\to\pm\infty$, there is only one zero of $G_{\pm}(\eta)$ on the positive real axis, and either zero or two on the negative real axis. The condition for two roots on the negative axis is that $G_{\pm}(-\sqrt{\zeta_{\pm}})\geqslant 0$, which reduces to (19). This may be rewritten as

$$(\zeta_{\pm}+1)(5\zeta_{\pm}+1)^3\zeta_{\pm}^{-3}\leqslant 16\ \epsilon_{\pm}^{-2}. \tag{20}$$

It can be easily checked that the left member has a unique minimum at $\zeta_{\pm}=1$, implying that (19) can only hold for systems with $\epsilon_{\pm}\leqslant\epsilon_c\equiv 1/\sqrt{27}=0.1925$, and then only for a range of subsonic frequencies, $0<\Omega_{\pm}^{l}\leqslant\Omega_{\pm}\leqslant\Omega_{\pm}^{u}\leqslant 1$ where $\Omega_{\pm}^{l}(\epsilon)<(12)^{-1/2}=0.2887<\Omega_{\pm}^{u}(\epsilon)$ are the values at which the equality holds.

Thus, one of the five $\theta_n^{\pm}$ lies on the negative imaginary axis, and either two or zero lie on the positive imaginary axis depending as (19) holds or not. For example, $\epsilon=0.134$ for steel and water, and $\epsilon = 0.4$ for aluminum and water, and consequently the latter system has only one purely imaginary θ_n, while steel and water has three for $0.0748 < \Omega_\pm < 0.5918$ and one otherwise. The ambiguity concerning the values of parameters $s_n^\pm = \mathrm{sgn}(\mathrm{Re}\,\theta_n^\pm)$ if $\mathrm{Re}X_n^\pm = 0$ can be removed by introducing a small amount of dissipation. Giving the bending stiffness $B_\pm$ a small negative imaginary part shifts these roots from the imaginary axis in the complex X plane to get $\mathrm{Re}X_{1,3,5}^\pm > 0$, $\mathrm{Re}X_{2,4}^\pm < 0$. Consequently, we have $\mathrm{Re}\,\theta_{1,3,5}^\pm \in (0, \pi/2)$, $\mathrm{Re}\,\theta_{2,4}^\pm \in (-\pi/2, 0)$ and $s_n^\pm = (-1)^{n-1}$, $n = 1,\ldots,5$. At very low frequency, such that $\Omega_\pm \ll 1$, asymptotic approximations to the roots yields $\theta_1^\pm \simeq -i\lambda_\pm$, $\theta_2^\pm \simeq -\theta_3^{\pm *} \simeq \theta_4^{\pm *} \simeq -\theta_5^\pm \simeq \theta_1^\pm - \frac{2}{5}\pi$, where $\lambda_\pm = -\frac{3}{5}\ln \Omega_\pm + \frac{1}{5}\ln \epsilon_\pm + \ln 2$. These limiting values specify the quadrant positions of the angles for finite $\Omega_\pm$. We note for future reference that $\mathrm{Im}\,\theta_2^\pm < 0$, $\mathrm{Im}\,\theta_4^\pm > 0$.

C. General solution of the functional equations

The general solution to Eq. (15) is represented as

$$S(\alpha) = \Psi(\alpha)\left(P_0 \frac{\sigma(\alpha,\phi_0)}{\Psi(\phi_0)} + \Lambda(\alpha)\right), \tag{21}$$

where $\Psi(\alpha)$, $\sigma(\alpha,\phi_0)$, and $\Lambda(\alpha)$ are each particular solutions to a pair of difference equations. Thus, $\Psi(\alpha)$ is the unique (up to a multiplicative constant) solution of the homogeneous system

$$L_\pm(\alpha)\Psi(\alpha \pm \Phi) - L_\pm(-\alpha)\Psi(-\alpha \pm \Phi) = 0, \tag{22}$$

which has no poles or zeros in the strip Π_0, $\sigma(\alpha,\phi_0)$ is the solution of the homogeneous system

$$\sigma(\alpha \pm \Phi, \phi_0) - \sigma(-\alpha \pm \Phi, \phi_0) = 0, \tag{23}$$

which has a simple pole with unit residue at the single point $\alpha = \phi_0$ in the strip Π_0, and $\Lambda(\alpha)$ is the particular solution of the nonhomogeneous system

$$\Lambda(\alpha \pm \Phi) - \Lambda(-\alpha \pm \Phi) = \frac{2\sin\alpha}{L_\pm(\alpha)\Psi(\alpha \pm \Phi)} \sum_{n=1}^{4} C_n^\pm \cos^{n-1}\alpha. \tag{24}$$

The function $\Psi(\alpha)$ is a product of special Malyuzhinets functions $\psi_\Phi(\alpha)$ which depends upon the Brewster angles for the boundaries, $\theta_n^\pm$, $n = 1,\ldots,5$. The form of $\Psi(\alpha)$ depends critically upon $s_n^\pm$, defined above, implying the following analytical form of the auxiliary function

$$\Psi(\alpha) = \frac{\Psi_1^+(\alpha)\Psi_3^+(\alpha)\Psi_5^+(\alpha)}{\Psi_2^+(\alpha)\Psi_4^+(\alpha)} \frac{\Psi_1^-(\alpha)\Psi_3^-(\alpha)\Psi_5^-(\alpha)}{\Psi_2^-(\alpha)\Psi_4^-(\alpha)}, \tag{25}$$

$$\Psi_n^\pm(\alpha) = \psi_\Phi\left(\alpha \pm \Phi + \frac{\pi}{2} + (-1)^n \theta_n^\pm\right) \times \psi_\Phi\left(\alpha \pm \Phi - \frac{\pi}{2} - (-1)^n \theta_n^\pm\right), \tag{26}$$

where $\psi_\Phi(\alpha)$ is the Malyuzhinets function, which is analytic for $|\mathrm{Re}\,\alpha| < 2\Phi + \pi/2$.

The required solution of the homogeneous system (23) is

$$\sigma(\alpha,\phi_0) = \frac{(\pi/2\Phi)\cos(\pi\phi_0/2\Phi)}{\sin(\pi\alpha/2\Phi) - \sin(\pi\phi_0/2\Phi)}. \tag{27}$$

Finally, the particular solution of (24) can be deduced as

$$\Lambda(\alpha) = \sum_{n=1}^{4} C_n^+ \Lambda_n^+(\alpha) + \sum_{n=1}^{4} C_n^- \Lambda_n^-(\alpha), \tag{28}$$

where the procedure to determine the functions $\Lambda_n^+(\alpha)$ is described in Appendix A, with the result

$$\Lambda_n^\pm(\alpha) = \mp \frac{1}{\pi i} \int_0^{i\infty} \frac{\sigma(\alpha, \beta \pm \Phi) \sin\beta \cos^{n-1}\beta}{L_\pm(\mp\beta)\Psi(\pm(\Phi - \beta))} d\beta. \tag{29}$$

In the limit as $\mathrm{Im}\,B_\pm \uparrow 0$, the point $\beta = -\theta_1^\pm$ lies on the contour of integration, resulting in a singularity of the integrand. This may be handled by taking the limit and evaluating the contribution as a principal value integral. A similar principal value contribution also occurs at $\beta = \theta_5^\pm$ when $\epsilon_\pm \leqslant \epsilon_c$ and $0 < \Omega_\pm^l \leqslant \Omega_\pm \leqslant \Omega_\pm^u < 1$. Such singularities located on the positive imaginary axis can be avoided by deforming the contour into the region $\mathrm{Im}\,\beta > 0$, $\mathrm{Re}\,\beta \in (0, \pi/2)$ where $1/\Psi(\pm(\Phi - \beta))$ by construction is regular and only one zero of $L_\pm(\mp\beta)$ occurs at $\beta = \theta_5^\pm$. In practice, the integration is performed numerically by deforming to the contour $L(N)$ which goes from 0 to x_0 to $x_0 + iN$, where $x_0 = \frac{1}{2}[\pi/2 + \mathrm{Re}(\theta_5^\pm)]$ and N need not be very large for fast convergence. The change of contour introduces a residue contribution at the circumscribed pole, thus

$$\Lambda_n^\pm(\alpha) = -\frac{2\sigma(\alpha, \theta_5^\pm \pm \Phi)\sin\theta_5^\pm \cos^{n-1}\theta_5^\pm}{L_\pm'(\mp\theta_5^\pm)\Psi(\pm(\Phi - \theta_5^\pm))} \mp \frac{1}{\pi i} \int_{L(\infty)} \frac{\sigma(\alpha, \beta \pm \Phi)\sin\beta \cos^{n-1}\beta}{L_\pm(\mp\beta)\Psi(\pm(\Phi - \beta))} d\beta. \tag{30}$$

The previous definitions of the functions $\Psi(\alpha)$ and $\Lambda(\alpha)$, and consequently $S(\alpha)$, are analytic only in the strip Π_0, but may be analytically continued outside this region by repeated use of the functional relations (15), (21), (22), and (24). For example, the values of these functions in the sectors neighboring Π_0, $\Pi_{\pm 1} = \{\alpha : \Phi < \mathrm{Re}(\pm\alpha) \leqslant 3\Phi\}$ are related to themselves in Π_0 by the formulas

$$\Psi(\alpha) = \frac{L_\pm(-\alpha \pm \Phi)}{L_\pm(\alpha \mp \Phi)} \Psi(-\alpha \pm 2\Phi), \quad \alpha \in \Pi_{\pm 1}, \tag{31}$$

$$\Lambda(\alpha) = \Lambda(-\alpha \pm 2\Phi) + \frac{2\sin(\alpha \mp \Phi)}{L_\pm(-\alpha \pm \Phi)\Psi(-\alpha \pm 2\Phi)} \times \sum_{n=1}^{4} C_n^\pm \cos^{n-1}(\alpha \mp \Phi), \quad \alpha \in \Pi_{\pm 1}, \tag{32}$$

$$S(\alpha) = \frac{L_\pm(-\alpha \pm \Phi)}{L_\pm(\alpha \mp \Phi)} S(-\alpha \pm 2\Phi) + \frac{2\sin(\alpha \mp \Phi)}{L_\pm(\alpha \mp \Phi)} \times \sum_{n=1}^{4} C_n^\pm \cos^{n-1}(\alpha \mp \Phi), \quad \alpha \in \Pi_{\pm 1}. \tag{33}$$

III. DETERMINATION OF CONSTANTS

The eight unknowns can be determined from a linear system of equations of the form

$$\begin{pmatrix} E_{11}^{+} & E_{11}^{-} & E_{12}^{+} & E_{12}^{-} & E_{13}^{+} & E_{13}^{-} & E_{14}^{+} & E_{14}^{-} \\ E_{21}^{+} & E_{21}^{-} & E_{22}^{+} & E_{22}^{-} & E_{23}^{+} & E_{23}^{-} & E_{24}^{+} & E_{24}^{-} \\ \vdots & \vdots & \vdots & \vdots & \vdots & \vdots & \vdots & \vdots \\ \vdots & \vdots & \vdots & \vdots & \vdots & \vdots & \vdots & \vdots \\ E_{81}^{+} & E_{81}^{-} & E_{82}^{+} & E_{82}^{-} & E_{83}^{+} & E_{83}^{-} & E_{84}^{+} & E_{84}^{-} \end{pmatrix} \begin{pmatrix} C_1^{+} \\ C_1^{-} \\ C_2^{+} \\ C_2^{-} \\ C_3^{+} \\ C_3^{-} \\ C_4^{+} \\ C_4^{-} \end{pmatrix}$$

$$=(g_1 \;\; g_2 \;\; g_3 \;\; g_4 \;\; g_5 \;\; g_6 \;\; g_7 \;\; g_8)^T. \tag{34}$$

The first four of these equations follow from certain regularity conditions on the integrand $S(\alpha)$, and the remaining four are consequences of the mechanical conditions at the vertex. The two sets of conditions are used below to determine the elements of $\mathbf{E}$ and $\mathbf{g}$.

A. Regularity conditions

The far-field ($r\rightarrow\infty$) behavior of the Sommerfeld integral (7) can be determined by deforming the contour γ into a pair of contours $\Gamma_\varepsilon(\pm\pi)$, one of which goes from $\pi-\varepsilon+i\infty$ through $\alpha=\pi$ to $\pi+\varepsilon-i\infty$, and the other is symmetric to it about the origin $\alpha=0$. Assuming that ε is positive and arbitrarily small, one finds that these contours belong totally to those portions of the complex α plane, labeled Π^{-}, in which $\mathrm{Im}\cos\alpha<0$, and hence any integral of $\exp(-ikr\cos\alpha)$ taken over the contours $\Gamma_\varepsilon(\pm\pi)$ vanishes as $r\rightarrow\infty$. In deforming the contour certain poles may be captured in the area designated as Π^{ess} which is enclosed by contours $\gamma_\pm$ at the top and bottom, and by $\Gamma_\varepsilon(\pm\pi)$ at the left and right. If the captured poles include one or more located inside the regions Π^{+} where $\mathrm{Im}\cos\alpha>0$, then the residues at such poles would grow exponentially with r, giving unphysical behavior at infinity. Poles of this type (named in Ref. 4 as ''forbidden'' poles) violate conditions at $r=+\infty$ for some $\phi\in(-\Phi,\Phi)$ and must be eliminated from the solution.

In the following we assume that $\mathrm{Im}\,\theta_2^{\pm}<0$, $\mathrm{Im}\,\theta_4^{\pm}>0$, then it can be shown that among the forbidden poles which are shared by Π^{ess} and Π^{+} are as follows: $\alpha=-\phi+\alpha_p^f$ where $p=1,2,3,4$, and

$$\begin{aligned} \alpha_1^f&=\theta_2^{+}+\pi+\Phi, \\ \alpha_2^f&=-\theta_4^{+}+\Phi, \\ \alpha_3^f&=-\theta_2^{-}-\pi-\Phi, \\ \alpha_4^f&=\theta_4^{-}-\Phi. \end{aligned} \tag{35}$$

In order to guarantee the correct behavior of the integral (7) as $r\rightarrow+\infty$ we have to cancel the residues of its transform $S(\alpha)$ at the forbidden poles (35) by equating

TABLE I. The junction conditions for clamped, free and hinged plates. In each case four of the eight unknowns are zero, and the remaining four are determined by four linear equations.

Type	Conditions	Implications	Equations
Clamped	$w_\pm(0)=0$, $w'_\pm(0)=0$	$C_3^{\pm}=C_4^{\pm}=0$	(40)
Free	$w''_\pm(0)=0$, $w'''_\pm(0)=0$	$C_1^{\pm}=C_2^{\pm}=0$	(41)
Hinged	$w_\pm=0$, $w''_\pm(0)=0$	$C_2^{\pm}=C_4^{\pm}=0$	(42)

$$P_0\frac{\sigma(\alpha_p^f,\phi_0)}{\Psi(\phi_0)}+\Lambda(\alpha_p^f)=0, \quad p=1,2,3,4\,. \tag{36}$$

These provide the first four rows of the matrix $\mathbf{E}$ and the vector $\mathbf{g}$. Thus,

$$g_p=-P_0\frac{\sigma(\alpha_p^f,\phi_0)}{\Psi(\phi_0)}, \quad p=1,2,3,4\,. \tag{37}$$

The elements of the top half of $\mathbf{E}$ follow by noting that the function $\Lambda(\alpha)$ satisfies the functional equations (24). Thus, $\alpha_1^f,\alpha_2^f\in\Pi_1$, $\alpha_3^f,\alpha_4^f\in\Pi_{-1}$ if $\Phi>\pi/2$ and consequently, using (32),

$$\begin{aligned} E_{pn}^{+}&=\Lambda_n^{+}(-\alpha_p^f+2\Phi) \\ &\quad+\frac{2\,\sin(\alpha_p^f-\Phi)\cos^{n-1}(\alpha_p^f-\Phi)}{L_+(-\alpha_p^f+\Phi)\Psi(-\alpha_p^f+2\Phi)}, \\ E_{pn}^{-}&=\Lambda_n^{-}(-\alpha_p^f+2\Phi), \quad p=1,2, \quad n=1,2,3,4, \end{aligned} \tag{38}$$

and

$$\begin{aligned} E_{pn}^{-}&=\Lambda_n^{-}(-\alpha_p^f-2\Phi) \\ &\quad+\frac{2\,\sin(\alpha_p^f+\Phi)\cos^{n-1}(\alpha_p^f+\Phi)}{L_-(-\alpha_p^f-\Phi)\Psi(-\alpha_p^f-2\Phi)}, \\ E_{pn}^{+}&=\Lambda_n^{+}(-\alpha_p^f-2\Phi), \quad p=3,4, \quad n=1,2,3,4. \end{aligned} \tag{39}$$

The functions $\Lambda_n^{\pm}(\alpha)$ and $\Psi(\alpha)$ in Eqs. (38) and (39) have arguments only in Π_0.

B. Junction conditions

1. Clamped, free, or hinged plates

We consider three sets of junction conditions under which the equations simplify considerably. These are listed in Table I as clamped, free, and hinged. In the former case both plates are clamped at the vertex, constraining motion there. The nonzero equations are

$$\begin{pmatrix} E_{11}^{+} & E_{11}^{-} & E_{12}^{+} & E_{12}^{-} \\ E_{21}^{+} & E_{21}^{-} & E_{22}^{+} & E_{22}^{-} \\ E_{31}^{+} & E_{31}^{-} & E_{32}^{+} & E_{32}^{-} \\ E_{41}^{+} & E_{41}^{-} & E_{42}^{+} & E_{42}^{-} \end{pmatrix} \begin{pmatrix} C_1^{+} \\ C_1^{-} \\ C_2^{+} \\ C_2^{-} \end{pmatrix} = \begin{pmatrix} g_1 \\ g_2 \\ g_3 \\ g_4 \end{pmatrix}. \tag{40}$$

Under "free" conditions the shear force and bending moment on each plate vanishes at the tip, and the equations are

$$\begin{pmatrix} E_{13}^{+} & E_{13}^{-} & E_{14}^{+} & E_{14}^{-} \\ E_{23}^{+} & E_{23}^{-} & E_{24}^{+} & E_{24}^{-} \\ E_{33}^{+} & E_{33}^{-} & E_{34}^{+} & E_{34}^{-} \\ E_{43}^{+} & E_{43}^{-} & E_{44}^{+} & E_{44}^{-} \end{pmatrix} \begin{pmatrix} C_3^{+} \\ C_3^{-} \\ C_4^{+} \\ C_4^{-} \end{pmatrix} = \begin{pmatrix} g_1 \\ g_2 \\ g_3 \\ g_4 \end{pmatrix}. \tag{41}$$

The hinged ends constrain the linear motion but not the rotation, and exert no moments, yielding

$$\begin{pmatrix} E_{11}^{+} & E_{11}^{-} & E_{13}^{+} & E_{13}^{-} \\ E_{21}^{+} & E_{21}^{-} & E_{23}^{+} & E_{23}^{-} \\ E_{31}^{+} & E_{31}^{-} & E_{33}^{+} & E_{33}^{-} \\ E_{41}^{+} & E_{41}^{-} & E_{43}^{+} & E_{43}^{-} \end{pmatrix} \begin{pmatrix} C_1^{+} \\ C_1^{-} \\ C_3^{+} \\ C_3^{-} \end{pmatrix} = \begin{pmatrix} g_1 \\ g_2 \\ g_3 \\ g_4 \end{pmatrix}. \tag{42}$$

2. Welded and forced

We now consider the important case of two plates that are mechanically joined at the vertex. The displacements and rotations are continuous, and there is an applied moment M_0 per unit length in the third dimension, and force $\mathbf{F}$ per unit length acting at the tip. The continuity conditions can be expressed in terms of the deflection $w_\pm(r)$ and their derivatives at $r=0$:[9]

$$\begin{aligned} & w'_+(0)+w'_-(0)=0\,, \\ & B_+ w''_+(0)-B_- w''_-(0)=M_0\,, \\ & \frac{B_\pm}{i\omega} w'''_\pm(0)+Z_\pm w_\pm(0)-\frac{(Z_+ + Z_-)}{\sin^2 2\Phi} \\ & \quad \times[w_\pm(0)+w_\mp(0)\cos 2\Phi]=\frac{F_r^\mp}{i\omega\ \sin 2\Phi}. \end{aligned} \tag{43}$$

Here, $F_r^\pm$ are the radial components of $\mathbf{F}$ along $\phi=\pm\Phi$. For acoustic or flexural wave incidence we have $M_0=0$ and $F_r^\pm=0$. Longitudinal waves traveling inwards towards the junction on the $\pm$plate can be considered by setting $M_0=0$ and

$$F_r^\pm=-2i\omega(Z_\pm U_0^\pm+Z_\mp U_0^\mp\ \cos 2\Phi), \tag{44}$$

where $U_0^\pm$ is the particle displacement of the incident longitudinal wave at $r=0$ in the radial direction, defined by (5). Using (16) implies

$$\begin{aligned} & \frac{C_3^+}{B_+}+\frac{C_3^-}{B_-}=0\,, \\ & C_2^+-C_2^-=-\frac{k^2}{2}M_0\,, \\ & \frac{k^2}{c}C_1^\pm+\frac{Z_\pm}{B_\pm}C_4^\pm-\frac{(Z_+ + Z_-)}{\sin^2 2\Phi}\left(\frac{C_4^\pm}{B_\pm}+\frac{C_4^\mp}{B_\mp}\cos 2\Phi\right) \\ & \quad =\frac{-ik^3F_r^\mp}{2c\ \sin 2\Phi}, \end{aligned} \tag{45}$$

and therefore the bottom half of $\mathbf{E}$ comprises zeros except for the elements

$$\begin{aligned} & E_{53}^\pm=\frac{\epsilon_\pm}{\Omega_\pm^3}, \quad E_{62}^\pm=\pm 1, \quad E_{71}^+=E_{81}^-=-\sin^2 2\Phi, \\ & E_{74}^+=\frac{\delta_+}{\Omega_+^2}\left(\cos^2 2\Phi+\frac{\epsilon_+\delta_-\Omega_-}{\epsilon_-\delta_+\Omega_+}\right), \\ & E_{74}^-=\frac{\delta_-}{\Omega_-^2}\cos 2\Phi\left(1+\frac{\epsilon_-\delta_+\Omega_+}{\epsilon_+\delta_-\Omega_-}\right), \\ & E_{84}^-=\frac{\delta_-}{\Omega_-^2}\left(\cos^2 2\Phi+\frac{\epsilon_-\delta_+\Omega_+}{\epsilon_+\delta_-\Omega_-}\right), \\ & E_{84}^+=\frac{\delta_+}{\Omega_+^2}\cos 2\Phi\left(1+\frac{\epsilon_+\delta_-\Omega_-}{\epsilon_-\delta_+\Omega_+}\right), \end{aligned} \tag{46}$$

while the right-hand members become for longitudinal incidence, using (44) and $M_0=0$,

$$\begin{aligned} & g_5=0, \quad g_6=0, \\ & g_7=(S_0^-+S_0^+\cos 2\Phi)\sin 2\Phi, \\ & g_8=(S_0^++S_0^-\cos 2\Phi)\sin 2\Phi. \end{aligned} \tag{47}$$

In summary, the right-hand side of the matrix equation (34) is defined by the incident pressures P_0 and $S_0^\pm$, and therefore all coefficients $C_n^\pm$ also have units of pressure.

IV. DIFFRACTED STRUCTURAL WAVES

The total longitudinal motion in the plates is defined by the displacement components in either plate in the radial direction:

$$u_\pm(r)=u_\pm^{\mathrm{inc}}(r)+u_\pm^{\mathrm{sc}}(r), \tag{48}$$

where $u_\pm^{\mathrm{inc}}(r)$ is the incident wave, from (6), and $u_\pm^{\mathrm{sc}}(r)$ is the scattered wave which satisfies

$$\omega k Z_\pm u_\pm^{\mathrm{sc}}(r)=A_L^\pm\ \exp(i\omega r/c_\pm), \tag{49}$$

indicating longitudinal energy radiating outwards. The initial amplitudes are related to the transverse displacements by[9]

$$u_\pm(0)=(\sin 2\Phi)^{-1}[w_\mp(0)+w_\pm(0)\cos 2\Phi], \tag{50}$$

and therefore, using (16), the longitudinal diffraction coefficients are

$$A_L^\pm=\frac{2\delta_\pm}{\Omega_\pm^2\sin 2\Phi}\left(C_4^\pm\ \cos 2\Phi+C_4^\mp\frac{\epsilon_\mp\Omega_\pm^3}{\epsilon_\pm\Omega_\mp^3}\right)-S_0^\pm. \tag{51}$$

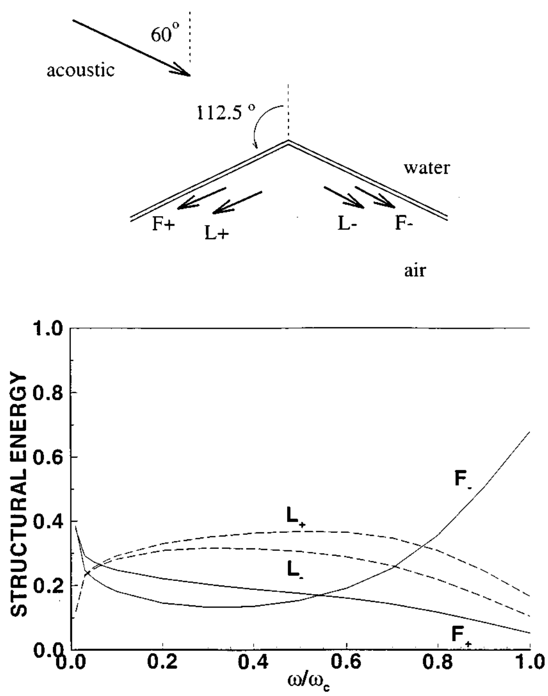

FIG. 2. The fraction of structural energy associated with flexural ($F_\pm$) and longitudinal ($L_\pm$) waves excited at the vertex of a steel and water configuration with $\Phi=112.5°$ for acoustic incidence at angle $\phi_0=60°$. The frequency ω_c is the flexural and acoustic coincidence frequency. The sum of the four energies is 1.

The evaluation of the flexural wave amplitudes requires a little more effort. The integral (7) can be evaluated asymptotically for $kr \gg 1$ by deformation of the contour γ into a pair of steepest descent paths. This yields a representation

$$p(r,\phi)=p_G(r,\phi)+p_D(r,\phi)+p_F^+(r,\phi)+p_F^-(r,\phi), \tag{52}$$

where p_G and p_D are the geometrical and acoustical (vertex) diffraction fields, respectively. The terms $p_F^\pm(r,\phi)$ denote the residues at captured poles of the function $\Psi(\alpha+\phi)$, and they coincide with the zeros of $L_\pm(\alpha+\phi\mp\Phi)$ which lie within the steepest descent paths. The dominant contributions to $p_F^\pm(r,\phi)$ are due to the residues at poles $\alpha=-\phi\pm(\Phi+\pi+\theta_1^\pm)$ that describe the subsonic flexural waves excited at the tip by the incident field and then traveling outwards along both sides of the wedge without dissipation if the material parameters of the plates are assumed to be entirely real, that is $\mathrm{Re}\,\theta_1^\pm=0$. The corresponding expressions may be summarized as follows

$$p_F^\pm(r,\phi)=H[\pm\phi-\Phi-\mathrm{Re}\,\theta_1^\pm - gd(\mathrm{Im}\,\theta_1^\pm)]A_F^\pm e^{ikr\cos(\Phi\mp\phi+\theta_1^\pm)}, \tag{53}$$

where gd is the Gudermanian function,[13] and using (33),

$$A_F^\pm=\frac{2}{L'_\pm(\theta_1^\pm)}\left(S(\pm\Phi\mp\pi\mp\theta_1^\pm) \pm\sin\theta_1^\pm\sum_{n=1}^{4} C_n^\pm \cos^{n-1}(\theta_1^\pm+\pi)\right). \tag{54}$$

The acoustical diffraction, p_D of (52), is defined by

$$p_D(r,\phi)\approx D(\phi)\frac{\exp(ikr-i3\pi/4)}{\sqrt{2\pi kr}}, \tag{55}$$

where the diffraction coefficient follows from a steepest descents integral as

$$D(\phi)=S(\phi+\pi)-S(\phi-\pi). \tag{56}$$

This term describes the cylindrical wave arising due to diffraction of the incident field by the tip. The acoustical diffraction coefficient must be unchanged under the interchange of the source and observation directions. Thus, when considered as a function of both ϕ and ϕ_0, it satisfies the reciprocity identity $D(\phi_0,\phi)=D(\phi,\phi_0)$.

The energy of an incident structural wave is defined as twice the flux of energy per cycle in the direction of the incoming wave. For the longitudinal wave this is simply the energy flux in the plate,

$$\mathscr{F}_L^\pm=\omega^2 Z_\pm |U_0^\pm|^2. \tag{57}$$

The flexural wave contains energy in the plate and in the fluid, and it can be shown to yield a flux of

$$\mathscr{F}_F^\pm=\frac{|L'_\pm(\theta_1^\pm)|}{2\rho\omega}|P_0|^2, \tag{58}$$

and $|L'_\pm(\theta_1^\pm)|=\pm iL'_\pm(\theta_1^\pm)$ assuming no dissipation in the system. The energy fluxes of the radiated flexural and longitudinal waves follow from (57) and (58), and the acoustic energy is

$$\lim_{r\to\infty}\frac{1}{\rho c}\int_{-\Phi}^{\Phi}|p_D(r,\phi)|^2 r\,d\phi=\frac{1}{2\pi\rho\omega}\int_{-\Phi}^{\Phi}|D(\phi)|^2 d\phi. \tag{59}$$

The total radiated energy, structural and acoustic, is therefore

$$\mathscr{F}_s=\frac{1}{2\rho\omega}\Bigg\{|L'_+(\theta_1^+)||A_F^+|^2+|L'_-(\theta_1^-)||A_F^-|^2 +\frac{2\epsilon_+|A_L^+|^2}{\delta_+\Omega_+}+\frac{2\epsilon_-|A_L^-|^2}{\delta_-\Omega_-} +\frac{1}{\pi}\int_{-\Phi}^{\Phi}|D(\phi)|^2 d\phi\Bigg\}. \tag{60}$$

This defines the energy balance for the wave conversion process.

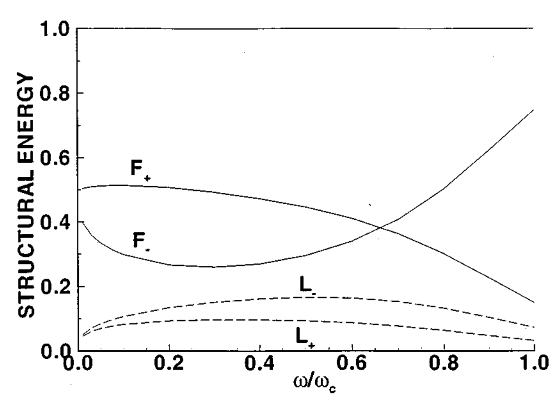

FIG. 3. The same as Fig. 2 but for $\Phi=135°$.

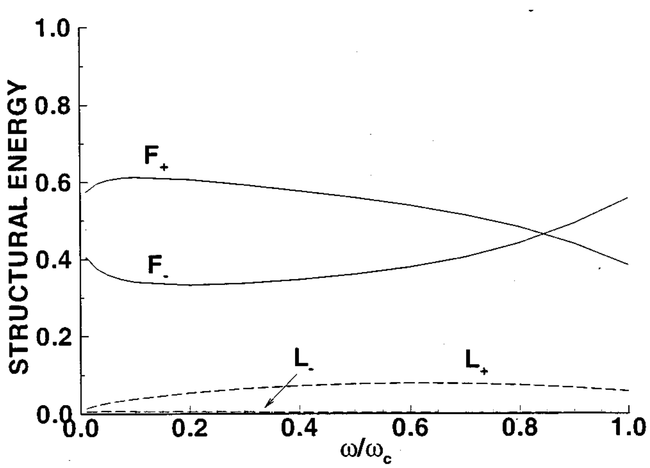

FIG. 4. The same as Fig. 2 but for $\Phi = 157.5°$.

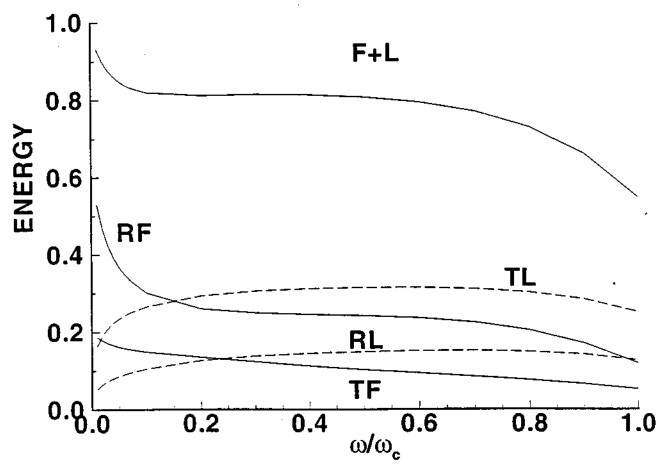

FIG. 6. The same as Fig. 5 for $\Phi = 157.5°$.

V. NUMERICAL RESULTS AND DISCUSSION

We now present some numerically computed results for the particular case of identical steel plates in water ($\epsilon = 0.134$) that are mechanically joined at the contact line (welded contact conditions). Several simplifications result when the plates are identical: thus, $\theta_n^+ = \theta_n^-$ for $n = 1,2,\ldots,5$, the function $\Psi(\alpha)$ is even,

$$\Lambda_n^+(\alpha) + \Lambda_n^-(-\alpha) = 0,$$

and

$$E_{1n}^{\pm} + E_{3n}^{\mp} = 0, \quad E_{2n}^{\pm} + E_{4n}^{\mp} = 0.$$

We consider three representative configurations: $\Phi = \frac{5}{8}\pi$, $\frac{3}{4}\pi$, and $\frac{7}{8}\pi$. Figures 2–8 show the energy partition for acoustical, flexural, and longitudinal incidence as a function of the nondimensional frequency $\Omega = \omega/\omega_c$.

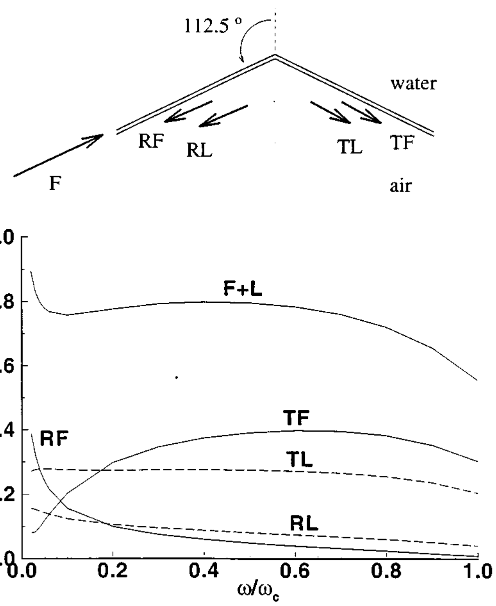

FIG. 5. The structural energy redistribution for flexural wave incidence on the steel and water configuration with $\Phi = 112.5°$. The curves ''RF,'' ''TF,'' ''RL,'' and ''TL,'' indicate the amounts of reflected flexural, transmitted flexural, reflected longitudinal, and transmitted longitudinal energies, respectively. The sum of these four energies is the curve ''F+L.''

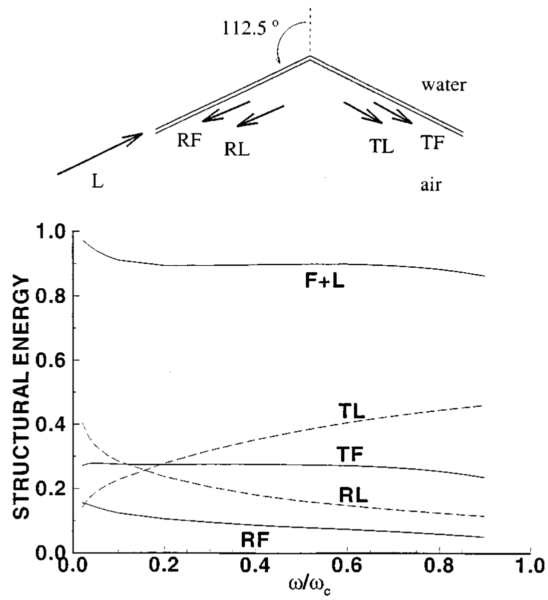

FIG. 7. The same as Fig. 5 but for longitudinal incidence.

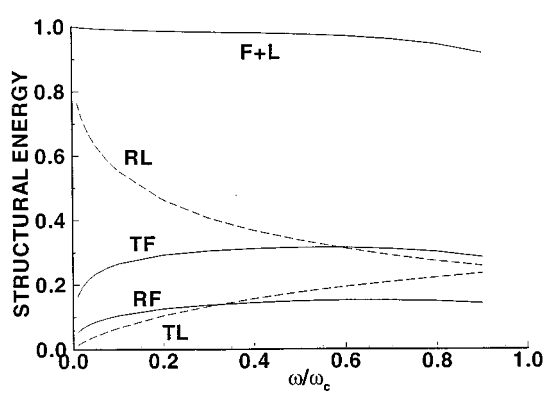

FIG. 8. The same as Fig. 7 for $\Phi = 157.5°$.

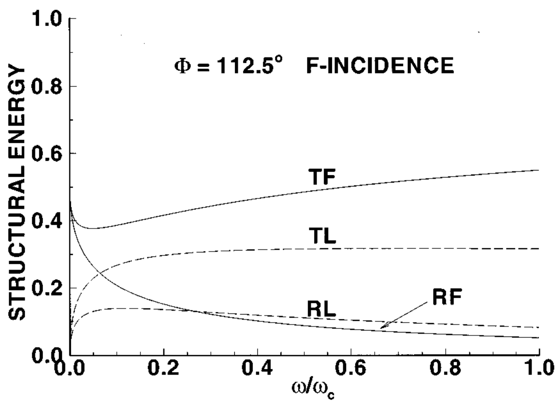

FIG. 9. The same as Fig. 5 but for dry plates (no fluid loading). The same frequency parameter is used for purposes of comparison. In this case the sum of the four fluxes is unity.

The fractional distribution of the diffracted structural energy for acoustic plane-wave incidence with $\phi_0 = 60°$ are shown in Figs. 2–4 for frequencies below critical. In these and subsequent plots the solid curves indicate the flexural energy and the dashed curves show the longitudinal energy fractions. We note from Figs. 2–4 that the relative coupling to flexural energy increases with the wedge angle, at the expense of the longitudinal energy which vanishes as $\Phi \to 180°$.

The curves in Figs. 5 and 6 show the fraction of incident flexural energy that is converted into the four radiating structural modes. In this case the sum of the flexural and longitudinal fluxes (the curve ''F+L'') is less than unity. The deficit indicates, from Eq. (60), the fraction of energy converted to acoustic waves. Similar curves for longitudinal incidence are in Figs. 7 and 8. In all cases the total structural energy is conserved at low frequency although it is significantly redistributed among the modes. These and other computations indicate that an incident longitudinal wave generates relatively little acoustic sound for all values of Φ considered, with most of its energy redistributed among structural modes. The acoustical diffraction is generally greater for flexural incidence.

Finally, Figs. 9 and 10 show the structural energy redistribution for two dry configurations (see Appendix B). These curves should be compared with the fluid-loaded cases in Figs. 5 and 8. It is interesting to note that the fluid loading does not have much effect for longitudinal incidence. The story is different for flexural incidence, where fluid loading effects can be appreciable for $\omega \leqslant 0.2\omega_c$. In general, experience shows (e.g., Ref. 11) that fluid loading has a strong influence on radiation and scattering from sources and discontinuities for $\Omega < \epsilon$, and the results presented here are consistent with this conclusion.

The numerical computations presented here indicate the degree of coupling between the modes for different wedge angles and frequencies. Some of the observed trends can be understood by consideration of the special cases (i): $\Phi = \pi$, for which a Wiener–Hopf analysis leads to relatively simple expressions for the acoustical and flexural diffraction coefficients,[7] and (ii) $\Phi \approx \pi/2$, which can be analyzed by perturbation methods,[9] with the flat plate $\Phi = \pi/2$ solution as the leading-order term. The latter analysis predicts that acoustic plane-wave incidence on flat junctions ($\Phi \approx 90°$) is converted almost equally, in terms of energy, among diffracted longitudinal waves on the two plates. This is in accord with the almost identical L_+ and L_- curves from the ''exact'' computations in Fig. 2.

ACKNOWLEDGMENT

The work of A. N. Norris was supported by the Office of Naval Research.

APPENDIX A: THE FUNCTION Λ

The general solution of the pair of difference equations

$$\Lambda(\alpha \pm \Phi) - \Lambda(-\alpha \pm \Phi) = f_\pm(\alpha), \tag{A1}$$

can be expressed as $\Lambda(\alpha) = \Lambda^+(\alpha) + \Lambda^-(\alpha)$, where

$$\begin{aligned} &\Lambda^+(\alpha+\Phi) - \Lambda^+(-\alpha+\Phi) = f_+(\alpha), \\ &\Lambda^+(\alpha-\Phi) - \Lambda^+(-\alpha-\Phi) = 0\,, \end{aligned} \tag{A2}$$

with a similar system for $\Lambda^-(\alpha)$. We will discuss the solution of the pair of simultaneous equations (A2) only, which apply to the functions Λ_n^+

The solution is represented using a modified Fourier transform pair:

$$\begin{aligned} &\Lambda^+(\alpha) = \int_{-i\infty}^{i\infty} e^{-i\alpha t}\eta(t)\,dt, \\ &\eta(t) = -\frac{1}{2\pi}\int_{-i\infty}^{i\infty} e^{i\alpha t}\Lambda^+(\alpha)\,d\alpha, \end{aligned} \tag{A3}$$

so that the difference equations (A2) become

$$\begin{aligned} &\int_{-i\infty}^{i\infty} [\eta(t)e^{-it\Phi} - \eta(-t)e^{it\Phi}]e^{-it\alpha}\,dt = f_+(\alpha), \\ &\int_{-i\infty}^{i\infty} [\eta(t)e^{it\Phi} - \eta(-t)e^{-it\Phi}]e^{-it\alpha}\,dt = 0. \end{aligned} \tag{A4}$$

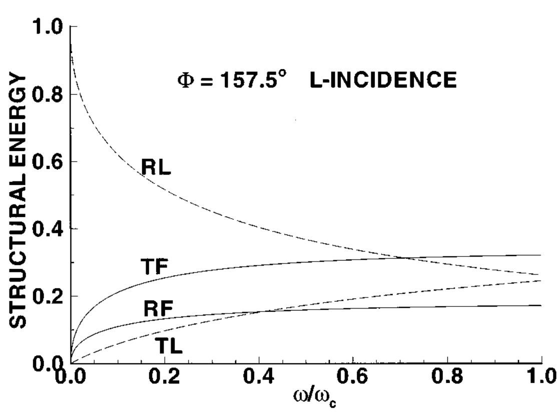

FIG. 10. The same as Fig. 8 but for dry plates.

Hence, using the modified Fourier transform, we easily obtain

$$\eta(t)=\frac{e^{-it\Phi}}{4\pi i\ \sin(2\Phi t)}\int_{-i\infty}^{i\infty}e^{i\beta t}f_+(\beta)d\beta, \tag{A5}$$

and so

$$\Lambda^+(\alpha)=\int_{-i\infty}^{i\infty}f_+(\beta)G(\beta,\alpha)d\beta, \tag{A6}$$

where

$$G(\beta,\alpha)=\int_{-i\infty}^{i\infty}\frac{e^{it(\beta-\Phi-\alpha)}dt}{4\pi i\ \sin(2\Phi t)}$$
$$=\int_{-i\infty}^{i\infty}\frac{\sin[(\beta-\Phi-\alpha)t]dt}{4\pi\ \sin(2\Phi t)}. \tag{A7}$$

But $f_+(\beta)$ is an odd function of its argument, implying that

$$\Lambda^+(\alpha)=\int_0^{i\infty}f_+(\beta)(G(\beta,\alpha)-G(-\beta,\alpha))d\beta, \tag{A8}$$

while

$$G(\beta,\alpha)-G(-\beta,\alpha)=\frac{i}{\pi}\int_0^{\infty}\frac{\sinh(\beta s)\cosh[(\alpha+\Phi)s)}{\sinh(2\Phi s]}ds$$
$$=\frac{i}{4\Phi}\,\frac{\sin(\beta\pi/2\Phi)}{(\cos(\beta\pi/2\Phi)-\sin(\alpha\pi/2\Phi)]}, \tag{A9}$$

where the latter follows from Eq. (3.511.5) of Ref. 13.

APPENDIX B: DRY PLATES

Consider incident flexural waves on the $\pm$ plate with displacement amplitudes $W_0^{\pm}$. The total transverse displacement on each plate can then be written as the sum of the incident wave plus outgoing propagating and evanescent flexural waves:

$$w_{\pm}(r)=W_0^{\pm}e^{-i\kappa_{\pm}r}+A_F^{\pm}W_0^{\pm}e^{i\kappa_{\pm}r}+B_F^{\pm}W_0^{\pm}e^{-\kappa_{\pm}r}. \tag{B1}$$

The following identities are direct consequences of (B1):

$$w''_{\pm}(0)+(1-i)\kappa_{\pm}w'_{\pm}(0)-i\kappa_{\pm}^2w_{\pm}(0)$$
$$=-2(1+i)\kappa_{\pm}^2W_0^{\pm}, \tag{B2}$$

$$w'''_{\pm}(0)+\kappa_{\pm}w''_{\pm}(0)+\kappa_{\pm}^2w'_{\pm}(0)+\kappa_{\pm}^3w_{\pm}(0)=0. \tag{B3}$$

The eight unknowns $w_{\pm}(0)$, $w'_{\pm}(0)$, $w''_{\pm}(0)$, $w'''_{\pm}(0)$, can now be found using the junction conditions (43) supplemented by (B2) and (B3).

We cite some results for the particular case of identical plates, with either flexural or longitudinal incidence, for which we find that

$$A_F^{\pm}=\frac{(1-i)}{2}w_s\pm\frac{1}{2}w_d+\frac{(1+i)}{2}W_0^{\mp}+\frac{(i-1)}{2}W_0^{\pm},$$
$$A_L^{\pm}=w_s\cot\Phi\mp w_d\tan\Phi-U_0^{\pm}, \tag{B4}$$

where $w_s=\frac{1}{2}[w_+(0)+w_-(0)]$, $w_d=\frac{1}{2}[w_+(0)-w_-(0)]$, or explicitly,

$$w_s=\frac{(U_0^++U_0^-)\cot\Phi+(1-i)(W_0^++W_0^-)\beta}{\cot^2\Phi+(1-i)\beta}, \tag{B5}$$

$$w_d=\frac{-(U_0^+-U_0^-)\tan\Phi+(W_0^+-W_0^-)\beta}{\tan^2\Phi+\frac{1}{2}(1-i)\beta}, \tag{B6}$$

with $\beta=\omega/(\kappa c_0)$ and c_0 is the longitudinal wave speed $(=c_{\pm})$. In terms of the nondimensional parameter Ω for the fluid loaded problem we have $\beta=\sqrt{\Omega}/\delta$. Finally, we note that the total energy balance for the dry plate problem is simply

$$|A_F^+|^2+|A_F^-|^2+\frac{1}{2\beta}|A_L^+|^2+\frac{1}{2\beta}|A_L^-|^2=1, \tag{B7}$$

for a single incident flexural wave of unit amplitude ($|W_0^+|$ or $|W_0^-|=1$), or for incidence of a longitudinal wave of amplitude $|U_0^+|$ or $|U_0^-|=\sqrt{2\beta}$. We refer to Budrin[14] and Maslov[15] for further results concerning the dry structural acoustics problem.

[1] A. N. Norris and G. R. Wickham, ‘‘Acoustic diffraction from the junction of two flat plates,’’ Proc. R. Soc. London **451**, 631–656 (1995).

[2] D. M. Photiadis, ‘‘Transport of energy across a discontinuity by fluid loading,’’ J. Acoust. Soc. Am. **97**, 1409–1414 (1995).

[3] D. A. Rebinsky and A. N. Norris, ‘‘Acoustic and flexural wave scattering from a three member junction,’’ J. Acoust. Soc. Am. **98**, 3309–3319 (1995).

[4] A. N. Norris, ‘‘Acoustic diffraction from the junction of two joined parallel plates,’’ J. Acoust. Soc. Am. **99**, 1475–1483 (1996).

[5] A. V. Osipov, ‘‘General solution for a class of diffraction problems,’’ J. Phys. A **27**, L27–L32 (1994).

[6] I. D. Abrahams and J. B. Lawrie, ‘‘Traveling waves on a membrane: reflection and transmission at a corner of arbitrary angle. I,’’ Proc. R. Soc. London **451**, 657–683 (1995).

[7] A. V. Osipov and A. N. Norris, ‘‘Sound diffraction by a fluid-loaded membrane corner,’’ Proc. R. Soc. London (in press).

[8] A. V. Osipov, ‘‘Sound diffraction by an angular joint of thin elastic plates,’’ Prikl. Mat. Mekh. (Russia) (in press).

[9] A. N. Norris and A. V. Osipov, ‘‘On acoustic interaction between two thin elastic plates through an angular welded joint,’’ J. Sound Vib. **196**, 75–84 (1996).

[10] G. D. Malyuzhinets, ‘‘Inversion formula for the Sommerfeld integral,’’ Sov. Phys. Dokl. **3**, 52–56 (1958).

[11] M. C. Junger and D. Feit, *Sound, Structures, and Their Interaction* (Acoustical Society of America, Woodbury, NY, 1993).

[12] D. G. Crighton, ‘‘The free and forced waves on a fluid-loaded elastic plate,’’ J. Sound Vib. **63**, 225–235 (1979).

[13] I. S. Gradshteyn and I. M. Ryzhik, *Table of Integrals, Series, and Products* (Academic, New York, 1980).

[14] S. V. Budrin and A. S. Nikiforov, ‘‘Wave transmission through assorted joints,’’ Sov. Phys. Acoust. **9**, 333 (1964).

[15] V. P. Masolv, ‘‘Reflection of a flexural wave from an angular junction of plates,’’ Sov. Phys. Acoust. **14**, 483–486 (1969).